Coating nanothickness degradable films on nanocrystalline hydroxyapatite particles to improve the bonding strength between nanohydroxyapatite and degradable polymer matrix

Heather L. Nichols,[1] Ning Zhang,[1,2] Jing Zhang,[2] Donglu Shi,[3] Sarit Bhaduri,[4] Xuejun Wen[1,2,5]
[1]*Clemson–MUSC Bioengineering Program, Department of Bioengineering, Clemson University, Charleston, South Carolina 29425*
[2]*Department of Cell Biology and Anatomy, Medical University of South Carolina, Charleston, South Carolina 29425*
[3]*Department of Chemical and Materials Engineering, University of Cincinnati, Cincinnati, Ohio 45221-0012*
[4]*Department of Materials Science and Engineering, Clemson University, Clemson, South Carolina 29634*
[5]*Department of Orthopedic Surgery, Medical University of South Carolina, Charleston, South Carolina 29425*

Received 16 March 2006; revised 15 June 2006; accepted 29 August 2006
Published online 12 February 2007 in Wiley InterScience (www.interscience.wiley.com). DOI: 10.1002/jbm.a.31066

Abstract: Hydroxyapatite (HA) nanoparticles are similar to bone apatite in size, phase composition, and crystal structure. When compared with micron-size HA particles, nano-HA possesses improved mechanical properties and superior bioactivity for promoting bone growth and regeneration. However, scaffolds fabricated from nano-HA alone cannot meet the mechanical requirements for direct-loading applications. A number of studies suggest that nanostructured composites may offer surface and/or chemical properties of native bone, and therefore represent ideal substrates to support bone regeneration. However, a common problem with nanohydroxyapatite (nano-HA)–polymer composites is the weak binding strength between the nano-HA filler and the polymer matrix since they are two different categories of materials and cannot form covalent bonds between them during the mixing process. Often, the mechanical strength of the composite is compromised due to the phase separation of the HA filler from the polymer matrix during the tissue repair process. To overcome this problem, an ultrathin degradable polymer film was grafted onto the surface of nano-HA using a radio-frequency plasma polymerization technology from acrylic acid monomers. The treated nano-HA powders are expected to bind to the polymer matrix via covalent bonds, thus enhancing the mechanical properties of the resultant composites. High-resolution transmission electron microscopy (HRTEM) experiments showed that an extremely thin polymer film (2 nm) was uniformly deposited on the surfaces of the nanoparticles. The HRTEM results were confirmed by X-ray photoelectron spectroscopy (XPS) and time-of-flight secondary ion mass spectroscopy (TOFSIMS). Tensile tests performed on the specimens revealed that the degradable coating had improved elastic and strength properties when compared with the nondegradable and uncoated controls. XPS and TOSIMS data revealed that more functional carboxyl groups were formed on degradable coatings than cross-linked nondegradable coatings. Cytocompatibility assay demonstrated that both the degradable and nondegradable coatings are cytocompatible. © 2007 Wiley Periodicals, Inc. J Biomed Mater Res 82A: 373–382, 2007

Key words: nanostructured materials; hydroxyapatite; coating; degradation; cytocompatibility; bone tissue engineering; mechanical properties

INTRODUCTION

Natural bone tissue possesses a nanocomposite structure interwoven in a three-dimensional (3D) matrix, which plays critical roles in conferring appropriate physical and biological properties to the bone tissue. For this reason, one single material may not be sufficient to mimic the composition, structure, and properties of native bone.

Hydroxyapatite (HA) has been used for bone repair and tissue engineering due to its biocompatibility, osteoconductivity, and osteoinductivity.[1–3] Through osteoconduction mechanisms HA can form chemical bonds with living tissue. However, its poor biomechanical properties (brittle, low tensile strength, high elastic modulus, low fatigue strength, and low flexibility), when compared with natural hard tissues, limit its applications to components of small, unloaded, or low-loaded implants, powders, coatings,

Correspondence to: X. Wen; e-mail: xjwen@clemson.edu
Contract grant sponsor:

composites, and so on. Nano-HA crystals are similar to bone apatite in size, phase composition, and crystal structure.[4,5] When compared with micron-size particles, nano-HA possess improved mechanical properties and superior bioactivity.[1,6,7] However, scaffolds fabricated from nano-HA alone still cannot meet the mechanical requirements for direct-loading applications, as well as application of dynamic force during the *in vitro* bone tissue engineering process.

As a result, both natural and synthetic polymeric materials have been studied extensively to overcome the mechanical problems with bioceramics for bone tissue engineering applications.[8–10] Aliphatic polyesters are an important class of biodegradable polymers for bone repair. Polylactic acid (PLA), polyglycolic acid (PGA), and their copolymer poly(dl-lactide-*co*-glycolide) (PLGA) have been well-studied for bone tissue repair and regenerations applications.[11–13] Despite a well-defined safety profile for biomedical applications, literature data have indicated that degradation through hydrolysis mechanisms may cause adverse effects, such as aseptic sinus, painful swell, and bone resorption surrounding the implant, possibly due to the release and accumulation of acidic degradation products in the local tissue.[14–16] Consequently, these implants exhibited excellent bone biocompatibility initially following implantation which then decreased dramatically as a function of implant degradation.[17] These polymers also undergo bulk degradation *in vivo* leading to the formation of voids inside the implant and a rapid deterioration in mechanical strength. To buffer the degradation products, bioceramics such as HA, calcium carbonate, sodium bicarbonate, tricalcium phosphate, and bioactive glass have been blended with polyesters at different ratios.[17,18]

The addition of nano-HA into the degradable polymeric matrix not only helped maintain the pH at nontoxic levels during degradation by neutralizing the acid degradation products of PLGA, but also enhanced the bone induction capacity of the scaffold. However, a common problem with HA–polymer composites is the weak binding strength between the nano-HA filler and the polymer matrix since they cannot form strong bonds during the mixing process. Often, the mechanical strength of the composite is compromised due to the phase separation of the HA filler from the polymer matrix. One way to overcome this is to coat the nano-HA with a polymer film (i.e. graft functional groups that are able to form strong bonds with the polymer matrix). The polymer coating needs be degradable so that the bioactivity of the nano-HA is not shielded. An ideal coating would be biocompatible, ultrathin, degradable, and form strong bonds with the polymer matrix. To this end, we have used radio-frequency plasma polymerization technology to activate nano-HA powder surfaces by creating a degradable film with functional groups (e.g., nano-HA-COOH) at nanoscale thickness.

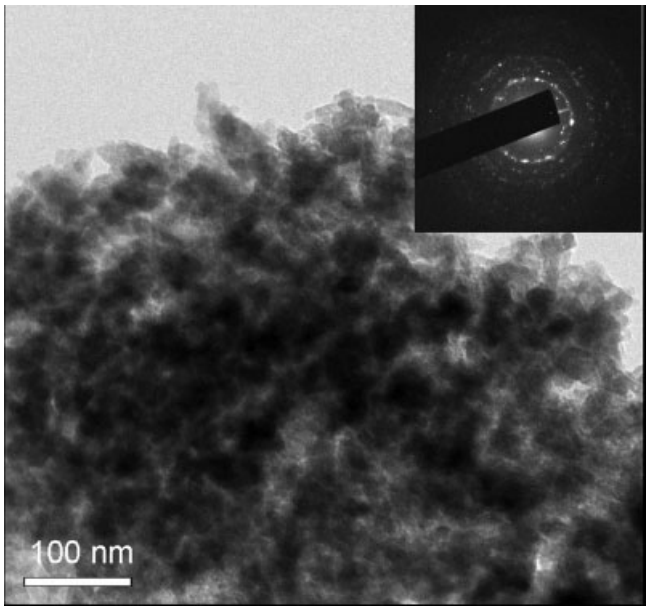

Figure 1. Morphology of nano-HA particles. Diffraction pattern shows nanocrystalline features (insert).

The purpose of this study is to improve the binding strength of the inorganic nano-HA filler and degradable polymer matrix by creating a nanothickness degradable film on the surfaces of nano-HA particles. PLGA was used as a model biodegradable polymer to demonstrate this concept. This technology can be applied to nano-HA blended with other types of biodegradable polymers as well.

MATERIALS AND METHODS

Nano-HA synthesis

Nanocrystalline hydroxyapatite (nano-HA), with average particle size 45 nm, was synthesized using a microwave-assisted "combustion synthesis (auto ignition)/molten salt synthesis" hybrid route as reported previously.[19] Aqueous solutions containing $NaNO_3$, $Ca(NO_3)_2 \cdot 4H_2O$, and KH_2PO_4 (with or without urea) were irradiated in a microwave for 5 min at 600 W of power. The as-synthesized precursors were then simply stirred in water at room temperature for 1 h to obtain the nano-HA particles (Fig. 1). The diffraction pattern shows nanocrystalline features (insert in Fig. 1).

Degradable polymer

PLGA 50/50 copolymers (M_w = 51,900; M_n = 34,000 and intrinsic viscosity = 0.2 dL/g; Birmingham Polymers, Birmingham, AL) was used as a model biodegradable polymer in this study. PLGA was purified prior to use.

The polymer was dissolved in tetrahydrofuran (5 g/dL), and the solution was slowly added to isopropanol (IPA) with continuous stirring. A volume ratio of 100 mL of polymer solution to 500 mL of IPA was not exceeded. The fibrous precipitate was then vacuum dried at room temperature for 48 h to remove solvent prior to use.

Nanothickness polymer coating on nano-HA powders

It is difficult to deposit thin films on nanoparticles using the plasma polymerization process because of the tendency of the nanoparticles to form aggregates,[20] where the unexposed regions of nanoparticles are barely modified. To successfully modify the surfaces of the nanoparticles, it is necessary to expose the entire surface of the nanoparticles to the plasma in the plasma deposition process. The fluidized-bed reactor is an ideal tool for gas-particle reactions since the nanoparticles are well dispersed in the reactor due to plasma oscillation, there is intensive mass and heat transfer between the two phases, a short reaction time, and a flat temperature profile. Furthermore, the combination of plasma polymerization and the fluidized-bed process is a suitable approach for the surface modification of nanoparticles. A homemade fluidized-bed reactor, as schematically shown in Figure 2, was used to create nanothickness coatings on the nano-HA particles. The body of the vacuum chamber of the fluidized-bed plasma reactor is a Pyrex glass column of about 50 cm in height and 6 cm in internal diameter. Nanoparticles are placed on the powder holder of a fine sieve. As the carrier gas/monomer vapor mixture flows through the sieve, nanoparticles are vigorously fluidized in the region above the sieve, where lies the center of the plasma that is produced by the RF generator through the connected coils. During this process, plasma polymerization of monomer occurs leading to the deposition of polymeric thin films onto the surfaces of the fluidized nanoparticles. Vigorous fluidization of nanoparticles in the plasma region allows homogenous coating of plasma polymerized thin films onto the nanoparticle surfaces. The operational parameters of the plasma reactor, such as the gas flow rate/reactor chamber gas pressure, the duration and the power of the plasma, the types of the carrier gas, the monomer and their mixing ratio, can be further controlled to achieve thin film polymer coatings of different properties on the nanoparticle surfaces. In this study, acrylic acid monomers (AA, >99%, Sigma-Aldrich) were used as starting materials. Low power and high gas pressure (15 W and 300 mTorr) condition was identified through a series of tests to create degradable films, and high power and low gas pressure (30 W and 80 mTorr) condition was identified to generate nondegradable coatings. The radio-frequency unit was operated at 13.56 MHz and an amplifier inductively coupled via an impedance matching unit and an external wound copper coil. A vapor delivery system was connected to the vacuum chamber to vaporize the liquid acrylic acid. The deposition time was 30 min.

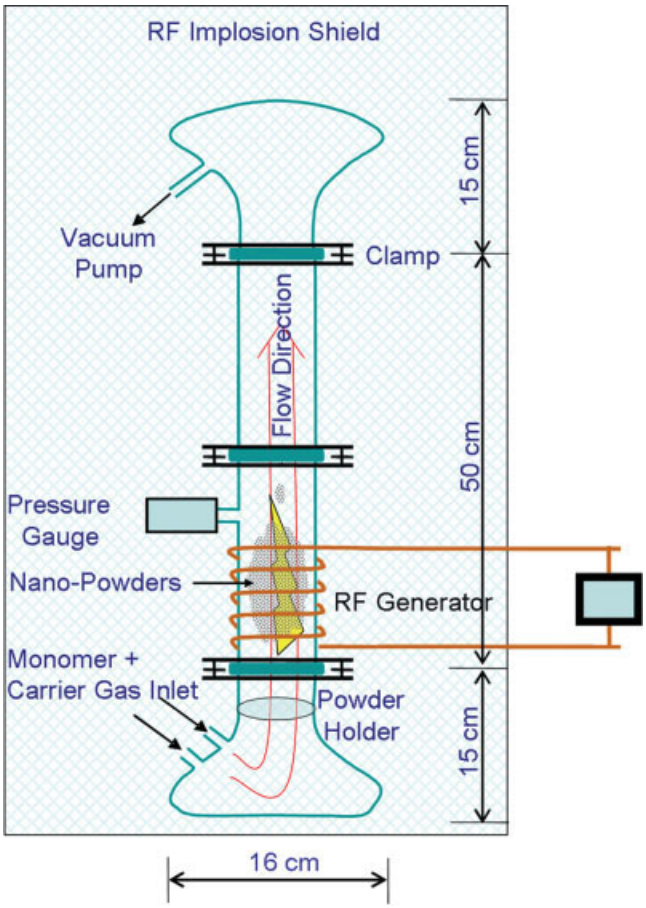

Figure 2. Schematic drawing shows the setup of a homemade fluidized-bed reactor, which mainly consists of an RF generator, long glass vacuum chamber, vacuum pump, and a pressure gauge. [Color figure can be viewed in the online issue, which is available at www.interscience.wiley.com.]

Degradation of the nanoscale coatings

Degradation of the nanofilm was studied using Fourier transform infrared (FTIR) before and after immersion in 0.1*M* PBS for 1–8 weeks. The experiments were carried out on a BIO-RAD FTS-40 instrument. The spectrum was obtained by the deduction of uncoated sample spectra as backgrounds.

Surface characterization of nanoscale coatings

Coated nano-HA particles were characterized using high-resolution transmission electron microscopy (HRTEM), energy dispersive X-ray (EDX) analysis, X-ray photoelectron spectroscopy (XPS), and time-of-flight secondary ion mass spectrometry (TOFSIMS). The HRTEM and EDX experiments were performed on a JEM 4000EX TEM. The chemical characterization of the coating was performed on an AXIS 165 XPS, ultra system and an ION-TOF Model IV TOFSIMS instrument. XPS was performed using a Mg K_a X-ray source. Wide scans (0–1200 eV) were used to obtain the surface oxygen:carbon ratio, while narrow scans were

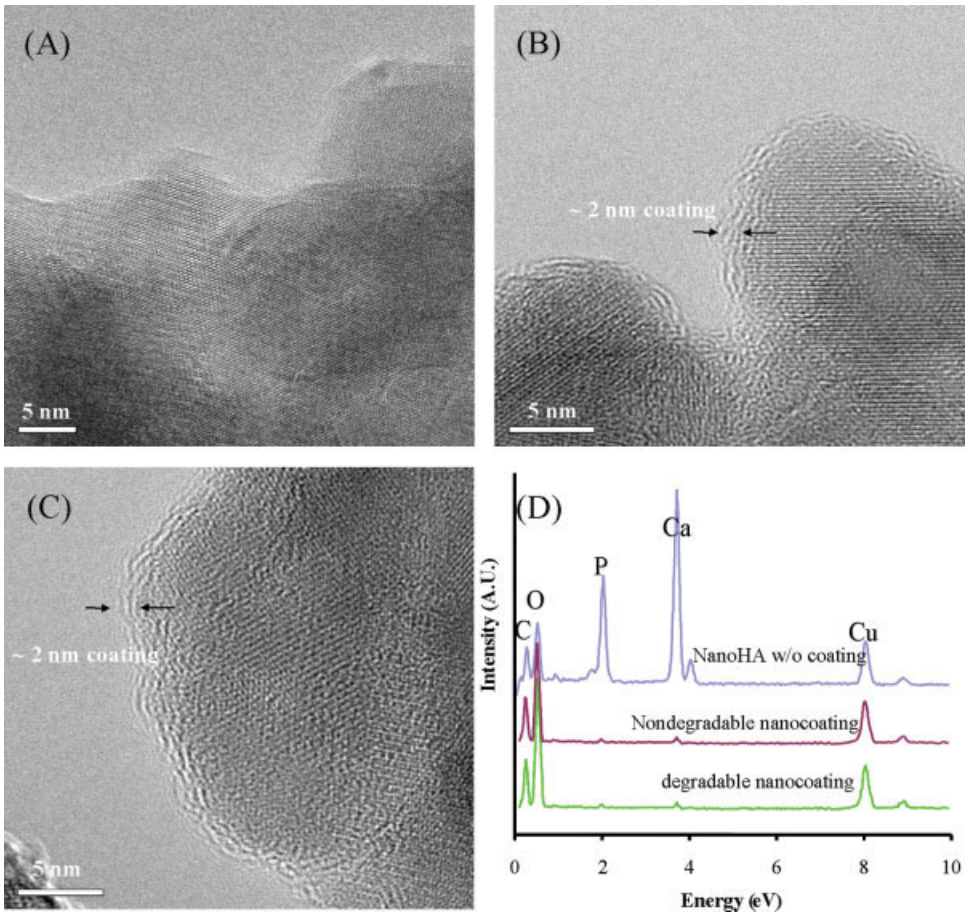

Figure 3. HRTEM images show the uncoated nano-HA (A), nano-HA with degradable coating (B), and nano-HA with nondegradable coating (C.). EDX curves (D) show the elements on the surface of nano-HA powders. [Color figure can be viewed in the online issue, which is available at www.interscience.wiley.com.]

used to determine the carbon- and oxygen-binding environment. A hydrocarbon peak was set to 285 eV to correct for sample charging.

Hydrophilicity test

Hydrophilicity of the coating was examined by measuring the water contact angle using a homemade microscopy based contact angle analyzer. For the ease of measurement, polymer coatings were deposited on clean glass slides.

Cytocompatability of coatings

Cytocompatibility of the coatings was examined with human osteoblasts (CRL-11372+) for 7 days *in vitro* using viability (trypan blue) and proliferation (MTT test) assays. In brief, 0.01 g coated or uncoated nano-HA powders were seeded on the bottom of 96-well plates filled with 1 mL 0.1*M* PBS. The plates are then centrifuged at 4000 rpm in an Eppendorf 5810R equipped with a rotor for microplate adaptors. After centrifugation, the nano-HA powders are spread on the bottom of the cell culture plates. Human osteoblasts (1×10^4) were seeded in each well and monitored for 7 days. The viability was tested using a trypan blue assay, and the proliferation was tested using a MTT assay.

Nano-HA–PLGA composite fabrication and mechanical testing

The nano-HA–PLGA composite strips were made using a solvent casting method. Briefly, 1.6 g of PLGA was fully dissolved in 40 mL acetone by constant stirring at room temperature for 24 h. Nano-HA powders (0.05 g) were well dispersed into the PLGA solution by vigorous mixing in an ultrasonic bath for 2 h. The mixture was then cast into a teflon mold that produces sheets, and air-dried at room temperature for 3 days followed by drying in a vacuum oven at room temperature for one additional day. The as-formed composite sheets were cut into strips of 6 mm wide, 50 mm long, and 0.15 mm thick in dimensions. Tensile tests were performed using a micromechanical testing machine (Vitrodyne Model 1000) with a crosshead speed of 125 mm/min.

Statistical analysis

Data were represented as the mean +/− the standard error of the mean for each group. Two-tail student's t-test was performed to determine the statistical significance using SPSSTM 9.0 software (SPSS, Chicago, Illinois). Statistical significance was accepted at $p < 0.05$.

RESULTS AND DISCUSSION

Figure 3 shows the HRTEM images of nano-HA with and without the nanothickness coatings. The coatings, ~2 nm thick, can be clearly seen. In the EDX analysis, the coatings were identified with HRTEM first, and then the element profile of the coating was obtained by EDX. The EDX curves for the nano-HA polymer coatings [Fig. 3(D)] indicate coverage of nano-HA particles with ultrathin carbon and oxygen based films. The phosphate (P) and calcium (Ca) peaks were reduced significantly, indicating the coverage of nano-HA particles with thin polymeric coatings.

The degradability of the coatings was examined using FTIR before and after immersion in 0.1 *M*PBS for 1–8 weeks. The FTIR curves in Figure 4 show that a soluble thin film was generated under low power and high pressure conditions, and a nonsoluble film was formed under high power and low pressure conditions. The disappearance of the peaks for the degradable coating indicates that the coating was dissolved after 2 weeks in culture. However, as the plasma power was increased from 15 to 30 W [Fig. 4(B)], the film remained after 8 weeks in culture. This indicates that highly cross-linked structures exist in the nondegradable coatings, which prevented the film from dissolving in culture.

The XPS wide survey showed only carbon and oxygen on the coating (Fig. 5). By comparing the oxygen:carbon ratio, the oxygen contents in the degradable coating were three times higher than that in the nondegradable coating, which indicates that nondegradable coatings were oxygen deficient. To calculate the carboxyl groups in the coating, peak deconvolution of the carbon spectrum was carried out to identify multiple carbon containing functionalities, followed by quantifying the contents of each functional group in the coating (Fig. 6). The C_{1s} core level spectrum, starting with the hydrocarbon (C-C/H) signal at 285 eV (Peak 1 in Fig. 6), and other four peaks β-shifted carbon C-COOH/R at 285.5 eV (Peak 2 in Fig. 6), alcohol/ether C-OH/R at 286.9 eV (Peak 3 in Fig. 6), carbonyl C=O at 287.9 eV (Peak 4 in Fig. 6), and carboxyl/carboxylate COOH/R at 289.35 eV were also found, respectively (Peak 5 in Fig. 6). The coatings contain 24.6% of COOH groups for the degradable coating and only 4.2% for the nondegradable coating.

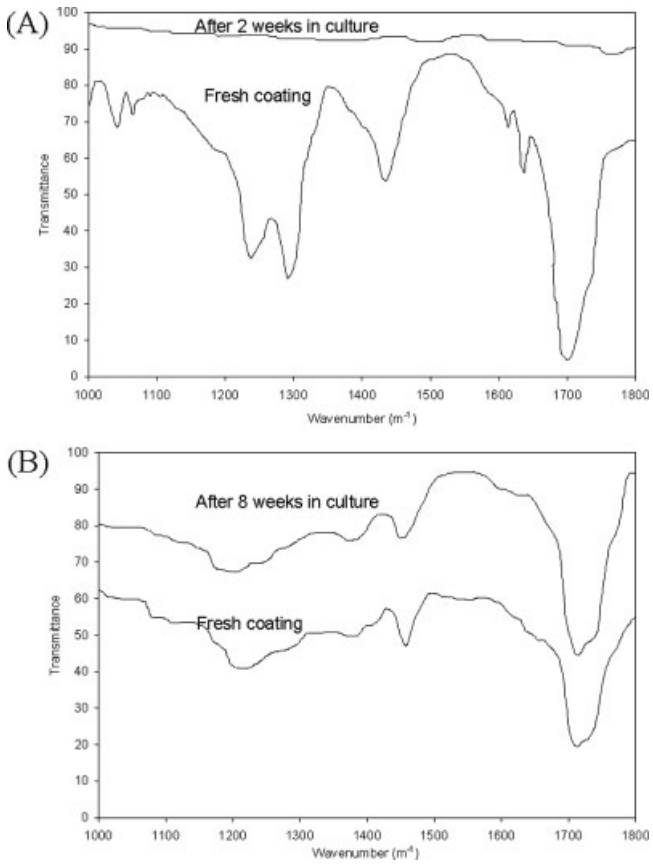

Figure 4. FTIR curves in (A) show the dissolution of the ultrathin film, created under 15 W and 300 mTorr, after 2 weeks in culture. FTIR curves in (B) show no dissolution of the thin film, generated under 30 W and 80 mTorr, after 8 weeks in culture.

Both positive and negative ion SIMS spectra of the coatings were studied to determine the chemical characteristics of the coatings. The negative ion spectra provided the most useful information in identifying the structure of the coating. SIMS data (Fig. 7) confirmed the EDX and XPS findings by showing more abundant carboxyl groups on the surface of degradable coatings than on the nondegradable coatings. Carboxyl groups act as a chemical "link" between the nano-HA and the polymer matrix as they are able to form covalent bonds. In the conventional polyacrylic acid (PAA), a single peak was present at m/z 71 in the m/z range of 40–80. However, in the plasma coated film, additional peaks were seen at m/z 45, 59, and 73. Those are either fragments or over polymerized structures of liner PAA.

Due to the fact that the coatings on the nano-HA particles were extremely thin (~2 nm), as demonstrated using HRTEM, surface sensitive techniques, such as XPS and SIMS, were utilized in the analysis of the elemental and functional composition of the coatings. Both XPS and TOSIMS elemental and functional composition analysis demonstrated significant

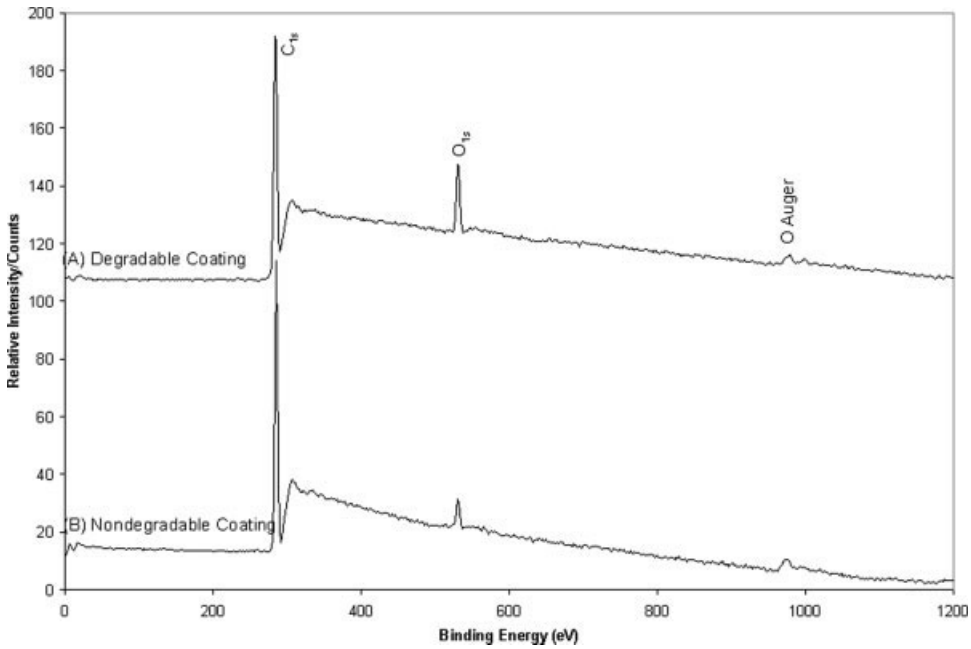

Figure 5. XPS wide survey from nanothickness coatings–(A) degradable coatings, and (B) nondegradable coatings.

differences in the functional composition between degradable and nondegradable coatings. As demonstrated in the XPS wide-survey of the coatings (Fig. 5), the oxygen content in the nondegradable coatings was three times less than that of the degradable coatings, which indicates the preferential incorporation of carbon into the coating and loss of oxygen in the form of gaseous products. Under high power conditions, monomers had the tendency to fragment under electron impact to form CO_2 and CO.[21] Therefore, the loss of oxygen content is related to the increased fragmentation of the monomer to form species that are not readily incorporated in the deposition.[22] The elemental and functional structure of the degradable coating is more close to the acrylic or PAA structure, as demonstrated in the XPS C_{1s} curve fitting plots shown in Figure 6(A). Hydrocarbon represents 64% of carbon and carboxyl groups represent 24.6%, and the remaining is represented by ester (6.4%) and ketone/aldehyde (5.4%). Therefore, the degradable coating is very similar to the conventional PAA or acrylic acid with the exception that about 6.4% of carbons have been converted into ester functionalities. In contrast, the nondegradable coating is highly cross-linked. The contents of hydrocarbon in the coating increased to 75.5%, ester contents increased to 12%, and ketone/aldehyde contents increase to 8.3%, while the carboxyl contents decrease to 4.2%. Therefore, under high power and low pressure conditions used in this study, the conversion of carboxyl groups into hydrocarbons, esters, or ketone/aldhydes is favorable, along with significant increases in cross-linking components. The nondegradable coating is very unlike acrylic acid or PAA, as it has a more cross-linked complex structure.

Plasma polymerization of acrylic acid has shown to provide highly functionalized surfaces with a high retention of monomer structure and high density of -COOH groups.[21,22] Our TOFSIMS data are in agreement with others' finding on the increment of OH and CO fragments with the increase of RF power. At low RF power, the fragmentation degree is minimalized and the COOH retention on the coatings is high. Therefore, by using low plasma power in creating degradable coatings, fragmentation can be kept to a minimum and the functional groups can also be preserved from over polymerization.[21,22]

Hydrophilicity of the coating was examined by measuring the water contact angle. The water contact angle was $(14.7 \pm 3.4)^\circ$ for the degradable coating and $(57.2 \pm 4.7)^\circ$ for the nondegradable coating. Hence, the degradable coatings were more hydrophilic than nondegradable coatings ($p < 0.05$). The increased hydrophilicity of the degradable coating is due to a higher percentage of functional COOH groups in the structure, when compared with the nondegradable coatings, as demonstrated using FTIR, XPS, and TOFSIMS.

Figure 8 shows the biocompatible nature of the nanothickness coatings. Both degradable and nondegradable thin films on the nano-HA surfaces were biocompatible. Adding the polymer coatings to the nano-HA did not significantly change the cytocompatibility of the nanoparticles or have proliferative effects on the human osteoblasts.

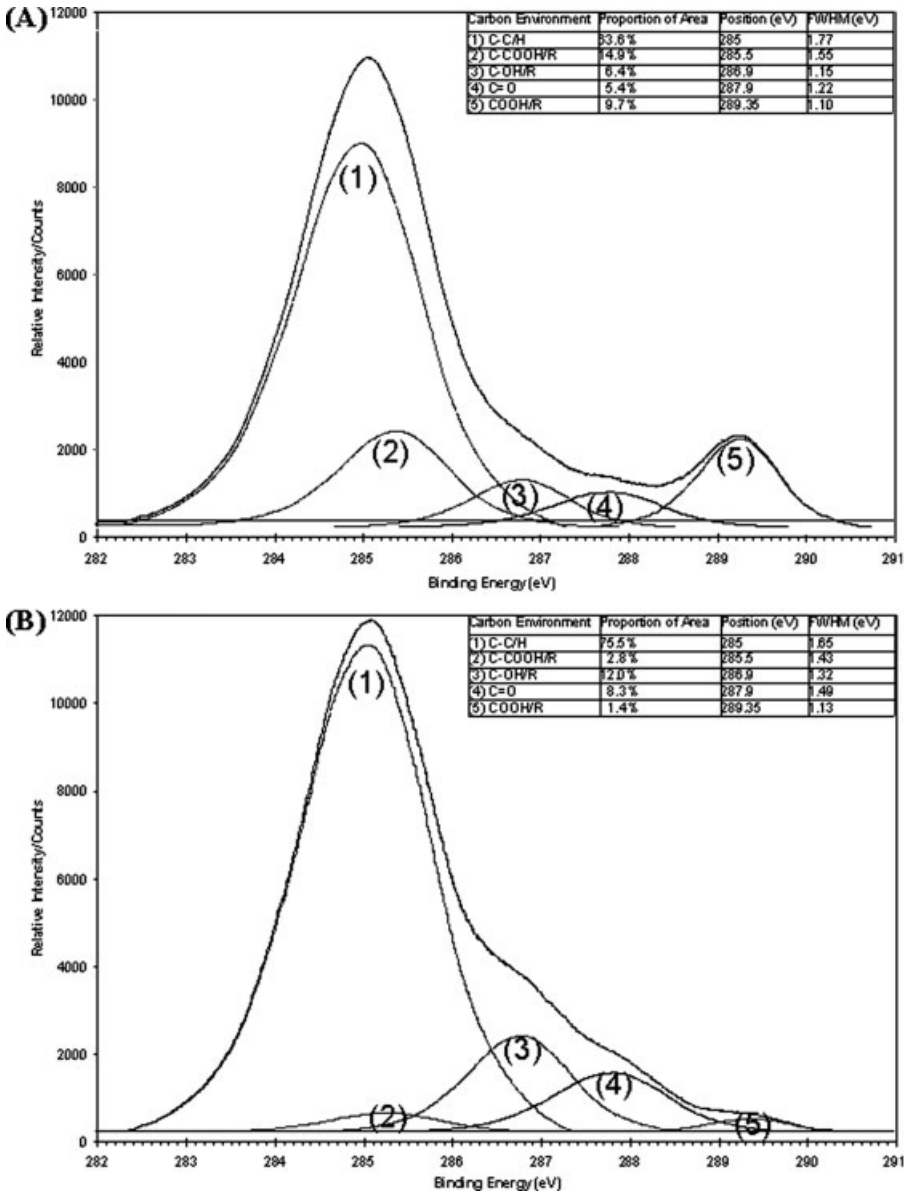

Figure 6. XPS C_{1s} peak from nanothickness coatings–(A) degradable coatings, and (B) nondegradable coatings.

Figure 9 shows three representative stress–strain curves for nano-HA doped PLGA scaffolds in thin sheet form. Nano-HA with the degradable coating showed the best mechanical properties when compared with uncoated and nondegradable coated nano-HA. The tensile strength and rupture strength [Fig. 10(A,B)] of the composite strips for the uncoated, degradable coated, and nondegradable coated nano-HA were calculated from stress–strain data. Both tensile strengths and rupture strengths are significantly different among the three groups. The tensile strengths are 0.67 ± 0.0351 MPa, 1.72 ± 0.0312 MPa, and 1.17 ± 0.1012 MPa for uncoated, degradable coating, and nondegradable coating samples, respectively. The rapture strengths are 0.64 ± 0.0538 MPa, 1.05 ± 0.0697 MPa, and 0.92 ± 0.0366 MPa for uncoated, degradable coating, and nondegradable coating samples, respectively. Young's (elastic) modulus [Fig. 10(C)] for the uncoated, degradable coated, and nondegradable coated nano-HA was 18.22 ± 2.8397 MPA, 51.17 ± 4.8009 MPA, and 32.54 ± 4.4896 MPa, respectively. Toughness [Fig. 10(D)] for the uncoated, degradable coated, and nondegradable coated nano-HA was 2.06 ± 0.5976, 2.67 ± 0.2268, and 1.56 ± 0.3999, respectively. The degradable coated nano-HA/PLGA composite had the highest elastic modulus, toughness, rupture strength, and tensile strength when compared to the nondegradable coated and uncoated nano-HA ($p < 0.05$).

Composite materials consisting of biomedical polymers, bioceramics, and other inorganic materials are good candidates for enhancing the mechanical prop-

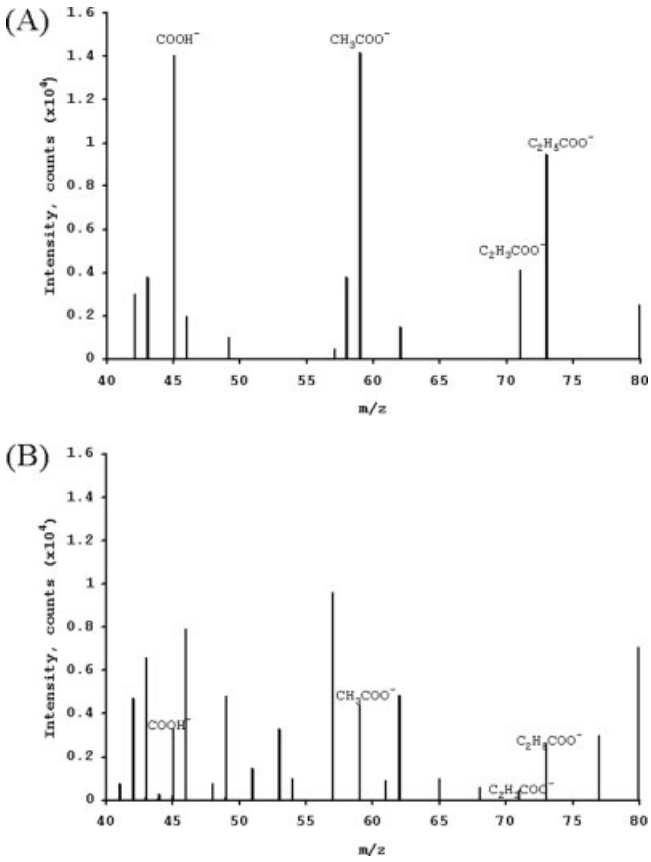

Figure 7. Representative TOFSIMS plots show strong signals of several types of carboxyl groups on the degradable nanofilm coated surface in (A), which may play as a chemical "link" in increasing the binding strength between the nano-HA particles and PLGA matrix. However, the signal intensity decreased dramatically in the nondegradable coatings (B).

erties of the bone tissue engineered scaffolds, hard tissue implants, and even dental filling composites. Among a variety of candidate materials, polymer–nanoparticle composites with superior mechanical properties, improved durability, and bioactivity appear most promising for these applications when compared with conventional polymer composites. For example, increased osteoblast and chondrocyte adhesion were observed on the surfaces of nanostructured PLGA/titania composites.[23] Seeded osteogenic cells into 3D porous scaffolds of nano-HA/collagen composites assumed morphologies similar to the ones in the normal bone tissue.[5] Enhanced bone tissue regeneration has been demonstrated on substrates of nano-HA/polymer composites as well.[5,23] A number of studies suggest that nanostructured composites may offer surface and/or chemical properties of native bone and cartilage, therefore, representing ideal substrates to support bone regeneration.[23] However, a common problem with HA–polymer composites is the weak binding strength between the HA filler and the polymer matrix since they are two different categories of materials and cannot form covalent bonds during the mixing process. Often, the mechanical strength of the composites is compromised due to the phase separation of the HA filler from the polymer matrix. To overcome this problem, we used radio-frequency plasma polymerization technology to activate nano-HA powder surfaces by grafting functional groups, such as carboxyl groups at nanoscale thickness from acrylic acid monomers. The treated nano-HA powders showed improved binding strength with the polymer matrix via covalent bonds, thus enhancing the mechanical properties of the resultant composites. The work presented here is just a proof of concept, and PLGA was used as a model degradable polymer. This fluid-bed based nanoparticle modification can be applied to almost all chemical natures of nanopowders to graft functional groups on their surfaces to improve adhesion with polymer matrix or for specific biomolecular conjugation.

Plasma deposition, or etching technique, is a powerful surface modification tool for many different areas of application, because it can be precisely controlled at a molecular level when combined with sophisticated *in situ* monitoring probes. Plasma pro-

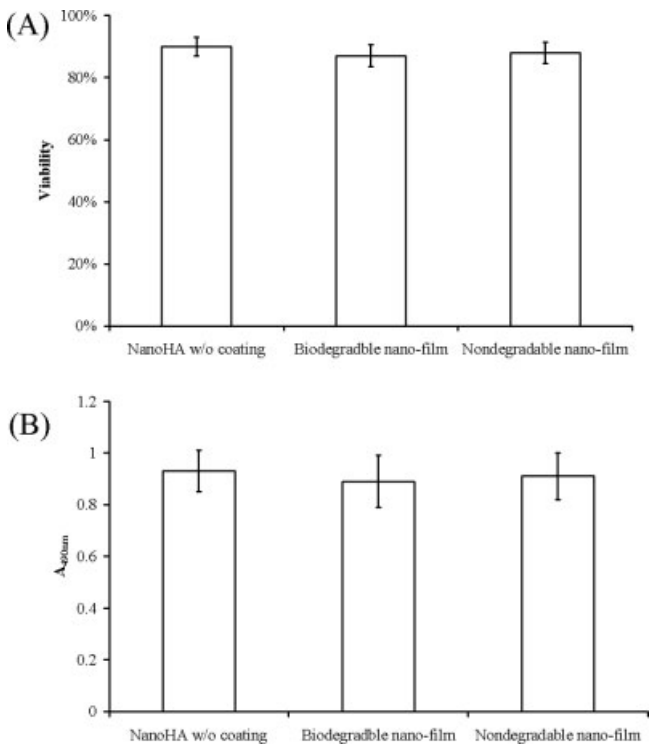

Figure 8. Viability (A) and proliferation (B) of human osteoblasts on nano-HA powder with or without coating showed no significant difference, which indicates that the nanothickness coating does not influence the cytocompatibility of the nano-HA powders. Error bars represent stand error of mean for $n = 7$.

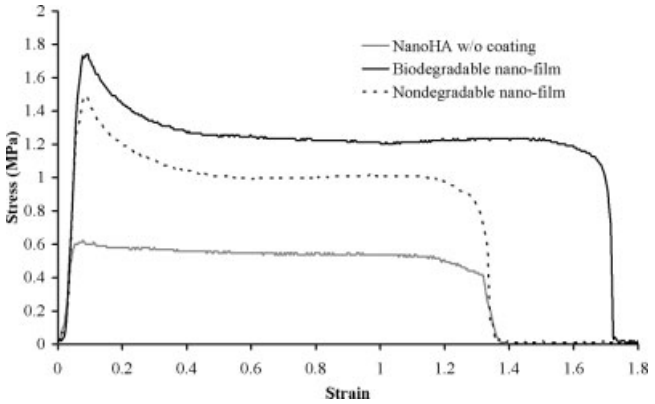

Figure 9. Representative stress–strain curves of nano-HA–PLGA strips. Nano-HA particles with degradable coatings show better mechanical properties than untreated nano-HA and nano-HA with nondegradable coatings ($n = 7$).

cessing techniques have already become mature techniques for the modification of the surfaces of bulk materials and macrosize particles or devices. Plasma polymerized organic layers have many advantages, such as strong adhesion to most substrates, excellent uniformity and thickness control, no pinhole formation, modification of only extreme superficial layers of the surface, and maintenance of the bulk material properties, etc. In addition, the elemental composition, chemical, and physical properties (such as surface energy) are easily controllable over a wide range. Many parameters can be adjusted to control the properties of the coating, including choosing suitable precursors, appropriate plasma conditions, such as power, pressure, and frequency of plasma driving field. For example, the selectivity, density, and mobility of the functional groups in the polymer coating can be varied by changing the degree of crosslinking. Therefore, the properties of the coating can be controlled to either degradable or nondegradable as described in this article. This is due to the fact that energy of the plasma radicals are comparable with chemical bond energies, and the radical density and energies can be controlled by plasma processing parameters, such as power, pressure, frequency, etc. Therefore, even the most inert substrates can be conveniently tailored. However, its applications in the surface modification of particles/powders at nanosize are not quite established due to their extremely small size. A plasma grafting process was utilized for the surface modification of nanoparticles, in this study, due to the attractive advantages for biomedical applications, including their ability to modify surface properties in a controlled manner without altering the bulk properties of the nanoparticles, and the possibility of scaling-up to industrial scale. To successfully modify the surfaces of the nanoparticles, it is necessary to expose the entire sur-

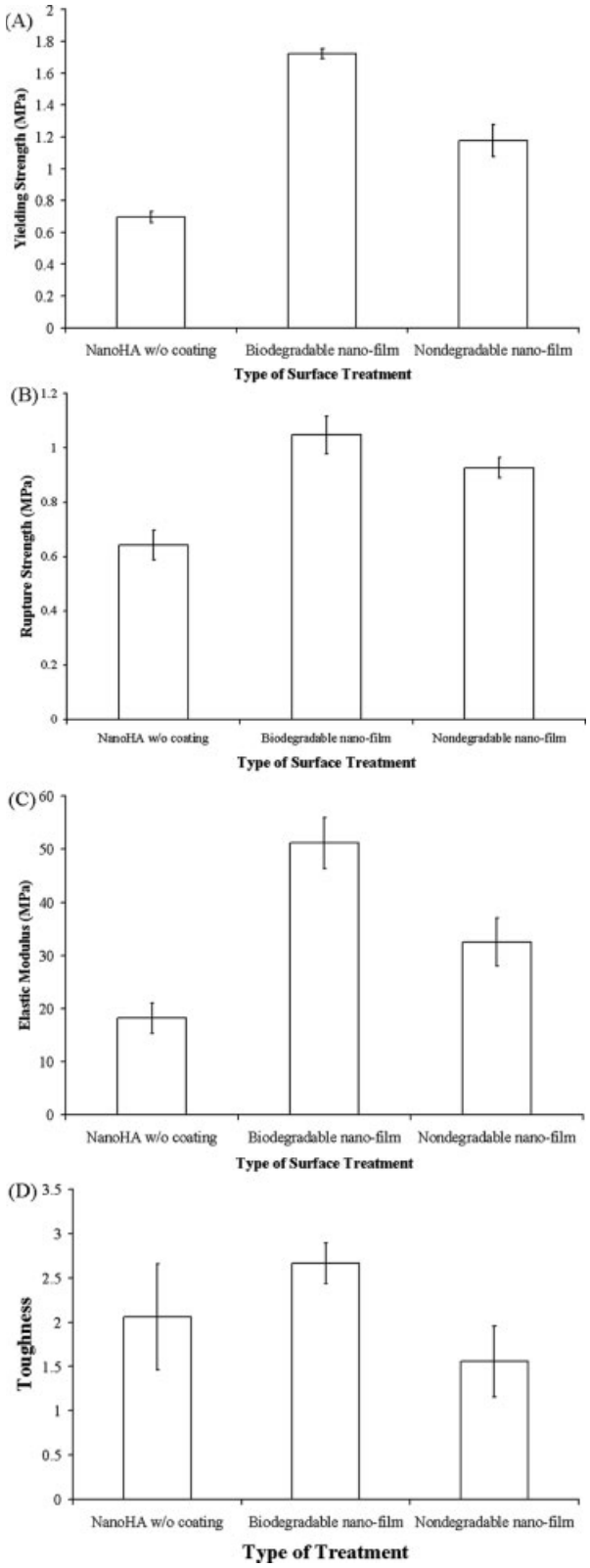

Figure 10. Yield strength (A), rupture strength (B), Young's modulus (C), and toughness of PLGA material mixed with nano-HA powders (10%) with or without coating showed a significant difference ($p < 0.05$), which indicates that the nanothickness degradable coating can increase the mechanical strength of the scaffold. Error bars represent standard error of mean for $n = 7$.

face of the nanoparticles to the plasma in the plasma deposition process. By combining the fluid-bed approach to avoid the tendency of the nanoparticles to form aggregates during the plasma polymerization, we were able to deposit ultrathin films on nanoparticles, which demonstrates that the fluidized-bed based plasma reactor is an ideal tool for gas-particle reactions since the nanoparticles are well dispersed in the reactor due to plasma oscillation.

CONCLUSION

Nanothickness films (1–2 nm) were grafted on nano-HA particles using a fluidized-bed RF reactor. By varying several parameters, such as monomer vapor pressure/flow rate, RF power, and pulse frequency, thin polymeric coatings with well controlled thickness, solubility, degree of cross-linking, chemical composition, and hydrophobicity can be achieved. Nanothickness films formed from acrylic acid monomers under 15 W and 300 mTorr can be dissolved *in vitro* for 2 weeks. The major functional groups of the degradable coating formed are carboxyl groups. The mechanical strength of the nano-HA–PLGA scaffold was significantly improved with ultrathin degradable coatings when compared with uncoated control and nondegradable nanocoated groups (30 W and 80 mTorr). The degradable ultrathin coating was also shown to be cytocompatible using viability and proliferation assays.

References

1. Wang X, Li Y, Wei J, de Groot K. Development of biomimetic nano-hydroxyapatite/poly(hexamethylene adipamide) composites. Biomaterials 2002;23:4787–4791.
2. Kikuchi M, Itoh S, Ichinose S, Shinomiya K, Tanaka J. Self-organization mechanism in a bone-like hydroxyapatite/collagen nanocomposite synthesized in vitro and its biological reaction in vivo. Biomaterials 2001;22:1705–1711.
3. Liao SS, Cui FZ. In vitro and in vivo degradation of mineralized collagen-based composite scaffold: Nanohydroxyapatite/collagen/poly(L-lactide). Tissue Eng 2004;10:73–80.
4. Itoh S, Kikuchi M, Takakuda K, Koyama Y, Matsumoto HN, Ichinose S, Tanaka J, Kawauchi T, Shinomiya K. The biocompatibility and osteoconductive activity of a novel hydroxyapatite/collagen composite biomaterial, and its function as a carrier of rhBMP-2. J Biomed Mater Res 2001;54:445–453.
5. Du C, Cui FZ, Zhu XD, de Groot K. Three-dimensional nano-HAp/collagen matrix loading with osteogenic cells in organ culture. J Biomed Mater Res 1999;44:407–415.
6. Sun TS, Guan K, Shi SS, Zhu B, Zheng YJ, Cui FZ, Zhang W, Liao SS. Effect of nano-hydroxyapatite/collagen composite and bone morphogenetic protein-2 on lumbar intertransverse fusion in rabbits. Chin J Traumatol 2004;7:18–24.
7. Du C, Cui FZ, Feng QL, Zhu XD, de Groot K. Tissue response to nano-hydroxyapatite/collagen composite implants in marrow cavity. J Biomed Mater Res 1998;42:540–548.
8. Lin AS, Barrows TH, Cartmell SH, Guldberg RE. Microarchitectural and mechanical characterization of oriented porous polymer scaffolds. Biomaterials 2003;24:481–489.
9. Kose GT, Korkusuz F, Korkusuz P, Purali N, Ozkul A, Hasirci V. Bone generation on PHBV matrices: An in vitro study. Biomaterials 2003;24:4999–5007.
10. Lahiji A, Sohrabi A, Hungerford DS, Frondoza CG. Chitosan supports the expression of extracellular matrix proteins in human osteoblasts and chondrocytes. J Biomed Mater Res 2000;51:586–595.
11. Li WJ, Laurencin CT, Caterson EJ, Tuan RS, Ko FK. Electrospun nanofibrous structure: A novel scaffold for tissue engineering. J Biomed Mater Res 2002;60:613–621.
12. Woo BH, Fink BF, Page R, Schrier JA, Jo YW, Jiang G, DeLuca M, Vasconez HC, DeLuca PP. Enhancement of bone growth by sustained delivery of recombinant human bone morphogenetic protein-2 in a polymeric matrix. Pharm Res 2001;18:1747–1753.
13. Tjia JS, Moghe PV. Regulation of cell motility on polymer substrates via "dynamic", cell internalizable, ligand microinterfaces. Tissue Eng 2002;8:247–261.
14. Bostman O, Pihlajamaki H. Clinical biocompatibility of biodegradable orthopaedic implants for internal fixation: A review. Biomaterials 2000;21:2615–2621.
15. Bostman O, Hirvensalo E, Makinen J, Rokkanen P. Foreign-body reactions to fracture fixation implants of biodegradable synthetic polymers. J Bone Joint Surg Br 1990;72:592–596.
16. Taylor MS, Daniels AU, Andriano KP, Heller J. Six bioabsorbable polymers: In vitro acute toxicity of accumulated degradation products. J Appl Biomater 1994;5:151–157.
17. Agrawal CM, Athanasiou KA. Technique to control pH in vicinity of biodegrading PLA–PGA implants. J Biomed Mater Res 1997;38:105–114.
18. Qiu QQ, Ducheyne P, Ayyaswamy PS. Bioactive, degradable composite microspheres: Effect of filler material on surface reactivity. Ann NY Acad Sci 2002;974:556–564.
19. Kutty MG, Loertscher J, Bhaduri S, Bhaduri SB, Tinga WR. Microwave sintering of nanocrystalline hydroxyapatite. Ceram Eng Sci Proc 2001;22:3–10.
20. Wen X, Shi D, Zhang N. Applications of nanotechnology in tissue engineering. In: Nalwa HS, editor. Handbook of Nanostructured Biomaterials and Their Applications. Stevenson Ranch, CA: American Scientific; 2005. pp 393–414.
21. O'Toole L, Beck AJ, Ameen AP, Jones FR, Short RD. Radiofrequency-induced plasma polymerisation of propenoic acid and propanoic acid. J Chem Soc Faraday Trans 1995;91:3907–3912.
22. Alexander MR, Duc TM. The chemistry of deposits formed from acrylic acid plasmas. J Mater Chem 1998;8:937–943.
23. Kay S, Thapa A, Haberstroh KM, Webster TJ. Nanostructured polymer/nanophase ceramic composites enhance osteoblast and chondrocyte adhesion. Tissue Eng 2002;8:753–761.